

Soft and Hard Pomerons

Uri Maor

*LAFEX, Centro Brasileiro de Pesquisas Físicas (CNPq)
Rua Dr. Xavier Sigaud 150, 22290 - 180, Rio de Janeiro, RJ, BRASIL*

and

*School of Physics and Astronomy
Raymond and Beverly Sackler Faculty of Exact Sciences
Tel Aviv University, Tel Aviv 69978, ISRAEL*

*Talk presented at the Theoretical Physics Symposium
in honor of Prof. Paulo Leal Ferreira*

Sau Paulo, SP, August 7-11,1995

ABSTRACT

The role of s-channel unitarity screening corrections, calculated in the eikonal approximation, is investigated for soft Pomeron exchange responsible for elastic and diffractive hadron scattering in the high energy limit. We examine the differences between our results and those obtained from the supercritical Pomeron-Regge model with no such corrections. It is shown that screening saturation is attained at different scales for different channels. We then proceed to discuss the new HERA data on hard (PQCD) Pomeron diffractive channels and discuss the relationship between the soft and hard Pomerons and the relevance of our analysis to this problem.

*Permanent address

Regge-pole theory was introduced into high energy physics some 35 years ago and was soon after followed by a very rich phenomenology[1]. The two key ingredients of this approach are the leading Regge trajectories

$$\alpha_R(t) = \alpha_R(0) + \alpha'_R t \quad (1)$$

where $\alpha_R(0) = 1 - \eta \simeq 0.5$ and $\alpha'_R \simeq 1 GeV^{-2}$.

These are accompanied by the Pomeron

$$\alpha_P(t) = \alpha_P(0) + \alpha'_P t \quad (2)$$

where we take a supercritical intercept $\alpha_P(0) = 1 + \Delta$ to account for the growing total cross sections. Whereas the Regge trajectories extrapolate nicely in the time like sector through the mesonic singularities (see Fig.1), the Pomeron is a more mysterious entity. Its existence is necessitated so as to maintain a self consistent theory and reproduce the high energy data. However, no mesonic singularities have been found in its time like sector. Also, in as much as the Pomeron plays a fundamental role in strong interactions, our understanding of its dynamics in terms of QCD is very partial at the best.

Regardless of the above reservations, we have seen, over the past few years, some very vigorous phenomenological investigations of the Pomeron through the study of forward elastic scattering and total cross sections. In particular, Donnachie and Landshoff (DL) have promoted [2] an appealing and very simple Regge picture in which

$$\sigma_{tot} = X \left(\frac{s}{s_0}\right)^\Delta + Y \left(\frac{s}{s_0}\right)^{-\eta} \quad (3)$$

with universal $\Delta = 0.0808$ and $\eta = 0.4525$, see Fig.2. This study is supplemented by the analysis of Block, Kang and White [3], who examine the nuclear slope of high energy pp and $\bar{p}p$ elastic scattering. They get an excellent reproduction of the data with $B = b_0 + 2\alpha'_P \ln(\frac{s}{s_0})$ where $\alpha'_P = 0.25 GeV^{-2}$. Even DL offer a global fit to all available hadron-hadron and photon-hadron total cross sections, it should be noted that in reality only $\bar{p}p$ and γp reactions have attained high enough energies in which the Pomeron parameters can be unambiguously tested, provided experimental errors are small enough.

Elastic scattering and diffraction dissociation are similar processes which have predominantly forward imaginary amplitudes corresponding to the exchange of vacuum quantum numbers in the t-channel. As such, both are dominated in the high energy domain by Pomeron exchange and are expected, in a simple Regge model, to exhibit rather similar dependences on the kinematic variables. Indeed, in the triple Regge limit we have for high enough energies

$$\frac{M^2 d\sigma_{sd}}{dM^2 dt} = \sigma_0^2 \left(\frac{s}{M^2}\right)^{2\Delta+2\alpha't} G_{PPP} \left(\frac{M^2}{s_0}\right)^\Delta \quad (4)$$

where $\sigma_0 = \sigma(s_0)$ and G_{PPP} is the triple Pomeron vertex couplings. The virtue of this formalism is that it makes a strong correlation between the energy dependences of σ_{tot} , σ_{el} and σ_{sd} , as well as with the mass dependence of σ_{sd} , i.e. $\frac{d\sigma_{sd}}{dM^2}$. The asymptotic predictions expected from a simple DL supercritical Pomeron model are summarized in the first column of Table I.

Table I. Asymptotic predictions of the Supercritical Pomeron and Eikonal models

	Supercritical Pomeron	Eikonal model
σ_{tot}	s^Δ	$\ln^2\left(\frac{s}{s_0}\right)$
σ_{el}	$\frac{s^{2\Delta}}{\ln\left(\frac{s}{s_0}\right)}$	$\ln^2\left(\frac{s}{s_0}\right)$
σ_{sd}	$\frac{s^{2\Delta}}{\langle \ln\left(\frac{s}{M^2}\right) \rangle}$	$\ln\left(\frac{s}{s_0}\right)$
$\frac{\sigma_{el}}{\sigma_{tot}}$	$\frac{s^\Delta}{\ln\left(\frac{s}{s_0}\right)}$	$\frac{1}{2}$
$\frac{\sigma_{sd}}{\sigma_{tot}}$	$\frac{s^\Delta}{\langle \ln\left(\frac{s}{M^2}\right) \rangle}$	$\frac{1}{\ln\left(\frac{s}{s_0}\right)}$
$\frac{d\sigma_{sd}}{dM^2}$	$(M^2)^{-(1+\Delta)}$	$(M^2)^{-(1+\Delta)}$

Clearly, the simple model we have presented is bound, eventually, to violate s-channel unitarity. This has obvious experimental consequences as $\frac{\sigma_{el}}{\sigma_{tot}}$ and $\frac{\sigma_{sd}}{\sigma_{tot}}$, which are expected to behave like s^Δ , cannot grow with energy indefinitely. The theoretical problems at stake are easily identified in an impact parameter b-space formalism which is outlined below.

Our amplitude is normalized so that

$$\frac{d\sigma}{dt} = \pi |f(s, t)|^2 \quad (5)$$

$$\sigma_{tot} = 4\pi \text{Im} f(s, 0) \quad (6)$$

The scattering amplitude in b -space is defined as

$$a(s, b) = \frac{1}{2\pi} \int d\mathbf{q} e^{-i\mathbf{q}\cdot\mathbf{b}} f(s, t) \quad (7)$$

where $t = -q^2$.

In this representation

$$\sigma_{tot} = 2 \int d\mathbf{b} \text{Im}a(s, b) \quad (8)$$

$$\sigma_{el} = \int d\mathbf{b} |a(s, b)|^2 \quad (9)$$

The properties of $a(s, b)$ are demonstrated in Fig.3. s -channel unitarity implies that $a(s, b) \leq 1$. This is actually just the black limit. We also have the analyticity/crossing limit. The position of this limit depends on the lightest relevant exchange we can make in the t -channel. Froissart[4], at the time, considered it to be a π meson. Our present thinking tends to consider it as the lightest glue-ball we can exchange. We can combine the two limits and obtain the well known Froissart bound[4]

$$\sigma_{tot} \leq C \ln\left(\frac{s}{s_0}\right) \quad (10)$$

where C depends on the exchanged mass.

Taking the DL parameters, it is an easy exercise to see that such a model will violate the unitarity limit for small b just above the present Tevatron energy. Indeed, CDF reports[5] that $a(b = 0, \sqrt{s} = 1800) = 0.96 \pm 0.04$. * The experimental problems associated with the simple supercritical Pomeron approach, outlined above, are demonstrated in Fig.4 and 5. In Fig.4 we see that $\frac{\sigma_{el}}{\sigma_{tot}}$ keeps growing through the ISR-Tevatron energy range, compatible with our simple expectations. This is not the case for $\frac{\sigma_{sd}}{\sigma_{tot}}$ which is lower in the Tevatron range than in the ISR range. This observation is further demonstrated in Fig.5 where we see that the ratio between the mass averaged $(\frac{d\sigma_{sd}}{dt})_{t=0}$ and $(\frac{d\sigma_{el}}{dt})_{t=0}$ goes down with energy. We are reminded that, by virtue of the factorization theorem, this ratio is just the ratio of the relevant coupling constants. As such, we expect it to approach, rather quickly, a constant value. Actually, since we average over M^2 , this ratio should increase very slowly with energy. The energy dependance shown in Fig.5 is very different. This ratio reaches its maximum at the ISR range and is decreasing rather rapidly at higher energies.

The purpose of this review is to demonstrate that the above difficulties, theoretical and experimental, can be resolved once we take into account the screening corrections necessitated by unitarity. Moreover, such a picture is very suggestive in a QCD motivated model where we wish to associate the total cross section growth with the small x increase of the projectiles gluon densities. In order to catalog the differences between a non screened supercritical Pomeron model and a similar model which includes screening corrections, let us specify their features side by side. I wish to present a model calculation which is reasonably realistic but also as simple as possible. To this end I present the Pomeron amplitude in an exponential form and calculate the screening corrections utilizing the eikonal approximation. This approximation accounts for elastic rescatterings which are the leading contribution to the screening process.

*To avoid this difficulty, DL have introduced a weak P-P cut correction which extends appreciably the domain of applicability of their model at the cost of Δ becoming eventually s dependant.

As stated, the introduction of screening rescattering corrections is greatly simplified in the eikonal approximation where at high energy $a(s, b)$ is assumed to be pure imaginary, and can be written in the simple form

$$a(s, b) = i(1 - e^{-\Omega(s, b)}) \quad (11)$$

where the opacity $\Omega(s, b)$ is a real function. As we shall utilize Regge parameterizations, analyticity and crossing symmetry are easily restored by substituting $s^\alpha \rightarrow s^\alpha e^{-i\pi\alpha/2}$, where α denotes the exchanged Regge trajectory.

In previous publications [6-8], we have shown that the eikonal approximation can be summed analytically for a Gaussian input

$$\Omega(s, b) = \nu(s) e^{-\frac{b^2}{R^2(s)}} \quad (12)$$

which corresponds to an exponential representation in t space. This is a good approximation for Regge type amplitudes where we get

$$\nu(s) = \frac{\sigma_0}{2\pi R^2(s)} \left(\frac{s}{s_0}\right)^\Delta \simeq \frac{\sigma_{tot}}{4\pi B_{el}} \quad (13)$$

$$R^2(s) = 4[R_0^2 + \alpha' \ln\left(\frac{s}{s_0}\right)] \quad (14)$$

where $\sigma_0 = \sigma(s_0)$ and $B_{el} = \frac{1}{2}R^2(s)$. With this input, we obtain in the eikonal approximation

$$\sigma_{tot} = 2\pi R^2(s)[\ln\nu(s) + C - Ei(-\nu(s))] \quad (15)$$

$$\sigma_{in} = \pi R^2(s)[\ln 2\nu(s) + C - Ei(-2\nu(s))] \quad (16)$$

$$\sigma_{el} = \sigma_{tot} - \sigma_{in} \quad (17)$$

where $Ei(x) = \int_{-\infty}^x \frac{e^t}{t} dt$, and $C = 0.5773$ is the Euler constant.

For the single diffraction channel with screening corrections we obtain[8]

$$\frac{M^2 d\sigma_{sd}}{dM^2} = \frac{\sigma_0^2}{2\pi \bar{R}^2(\frac{s}{M^2})} \left(\frac{s}{M^2}\right)^{2\Delta} G_{PPP}\left(\frac{M^2}{s_0}\right)^\Delta a \frac{1}{(2\nu(s))^a} \gamma(a, 2\nu(s)) \quad (18)$$

where

$$\bar{R}^2\left(\frac{s}{M^2}\right) = 2R_0^2 + r_0^2 + 4\alpha' \ln\left(\frac{s}{M^2}\right) \quad (19)$$

$r_0 \leq 1\text{GeV}^{-2}$ denotes the radius of the triple vertex and can safely be neglected.

$$a = \frac{2R^2(s)}{\bar{R}^2(\frac{s}{M^2}) + 2\bar{R}^2(\frac{M^2}{s_0})} \quad (20)$$

$\gamma(a, 2\nu)$ denotes the incomplete Euler gamma function $\gamma(a, 2\nu) = \int_0^{2\nu} z^{a-1} e^{-z} dz$. In the high energy limit the above expression simplifies to

$$\frac{M^2 d\sigma_{sd}}{dM^2} = \pi R^2(s) \left[G_{PPP}\left(\frac{M^2}{s_0}\right)^\Delta + G_{PPR}\left(\frac{M^2}{s_0}\right)^{-\frac{1}{2}} \right] \quad (21)$$

The remarkable differences between the non screened and eikonalized versions of the supercritical Pomeron model are best illustrated in the asymptotic region and are summarized in Table I. As can

be readily seen, the most dramatic change takes place for single diffraction where a $s^{2\Delta}$ divided by a lns term is replaced by $R^2(s)$ which behaves as lns . Problem is that the Value of ν in the ISR-HERA-Tevatron energy range is of the order of unity, which means that we are well below the asymptotic region. Consequently, the information summarized in Table I, as interesting as it may be, is of no practical use as long as we do not specify the appropriate energy scales at which the screening corrections saturate and become appreciable.

To this end we define a damping factor[9]

$$D^2 = \frac{\sigma_i[\text{with SC}]}{\sigma_i[\text{with no SC}]} \quad (22)$$

which reads for σ_{tot} and σ_{el}

$$D_{tot}^2 = 1 - \sum_{n=1}^{\infty} (-1)^{n+1} \frac{\nu^n}{(n+1)^2 n!} \quad (23)$$

$$D_{el}^2 = 1 - 4 \sum_{n=1}^{\infty} (-1)^{n+1} \frac{\nu^n (2^{n+1} - 1)}{(n+2)^2 (n+1)!} \quad (24)$$

For the inelastic channels the damping factor is defined

$$D^2 = \frac{\int d\mathbf{b} a_i(s, b) P(s, b)}{\int d\mathbf{b} a_i(s, b)} \quad (25)$$

where $a_i(s, b)$ is the b-space amplitude of interest, and $P(s, b) = e^{-2\Omega(s, b)}$ denotes the probability that no inelastic interaction takes place at impact parameter b .

For $M^2 \frac{d\sigma_{sd}}{dM^2}$ we get

$$D_{sd}^2 = 1 - a \sum_{n=1}^{\infty} (-1)^{n+1} \frac{(2\nu)^n}{(n+a) n!} \quad (26)$$

where a was defined in Eq.(20).

The damping parameters in the ISR-Tevatron energy range have been studied in detail in Ref.[9]. The important conclusion reached is that the above energy range is too low so as to enable an assessment of the importance of the screening corrections in total and elastic cross sections. The success of the DL model is thus understood. The emerging picture is that we expect $\frac{\sigma_{el}}{\sigma_{tot}}$ to start its rise, behaving approximately as s^Δ , and at the energy scale where screening becomes important to temper its rise approaching $\frac{1}{2}$ from below at exceedingly high energies.

On the other hand, a careful study[8,9] shows that the scale at which screening saturates for the diffractive channels is appreciably lower, about $\sqrt{s} \simeq 50 - 100 \text{ GeV}$. This is, indeed, the scale suggested by the SD data shown in Figs.4 and 5. This is compatible with the Pumplin bound[10]

$$\frac{\sigma_{el} + \sigma_{diff}}{\sigma_{tot}} \leq \frac{1}{2} \quad (27)$$

Our remarkable conclusion is that whereas we have not reached, as yet, the screening saturation scale corresponding to elastic $\bar{p}p$ scattering, the single diffraction scale is considerably smaller at c.m. energies of about 50-100 GeV. Consequently, SD cross sections behave differently than the elastic cross sections above an energy scale which is in the 50-100 GeV range.

A very exiting new window of information through which we can examine our ideas on Pomeron physics, has been opened recently when the second generation of HERA results became available. Actually, we have two avenues of new knowledge. To begin with, and as we have already noted, real photoproduction is the only channel, in addition to $\bar{p}p$, where our c.m. energies exceed 100 GeV. Clearly, a very important element in non screened Regge models is the universality of Δ . The analysis of the global data on $\sigma_{tot}(\gamma p)$ and $\sigma(\gamma p \rightarrow \rho p)$, including the HERA points, is therefore crucial for our understanding of the role of screening below saturation in soft Pomeron processes[11].

On a more profound level, we should re-assess what do we actually mean when we refer to the "Pomeron". Our discussion, thus far, was confined to soft processes, within the domains of conventional Regge physics. In PQCD a hard Pomeron, called the BFKL Pomeron, can be perceived[12] through the summation of gluon ladder diagrams. As a result, we obtains a series of poles in the complex j plane above unity. These poles sum to an effective $\Delta = \frac{12}{\pi} \alpha_s \ln 2$. Inserting a reasonable value for α_s we get $\Delta \simeq 0.5$ which seems, at first sight, rather high. It is, therefor, convenient to re define the Pomeron as an effective exchange with no colour flow, which has therefor a clean experimental signature of a large rapidity gap. Such a definition is compatible with both the Regge soft and the BFKL hard Pomerons. The above definition leaves opened the more fundamental problem of the relationship and transition between the soft and hard phenomena associated with the "Pomeron". We shall return to this after reviewing the relevant data.

A unique property of HERA is that its kinematics are such that we can explore Pomeron physics in domains that are accessible to PQCD calculations. Since at very small x , $\sigma_{tot}(\gamma^* p) = \frac{4\pi^2\alpha}{Q^2} F_2(x, Q^2)$, we can actually carefully scan the experimental dependence of Δ on Q^2 . We are reminded that a pre HERA analysis by ALLM[13] of $F_2(x, Q^2)$ predicted a fast variation of Δ as a function of Q^2 . Namely, ALLM obtain a $\Delta \leq 0.1$ at $Q^2 \leq 1 \text{ GeV}^2$ which is changing to $\Delta \simeq 0.4$ at $Q^2 \geq 10 \text{ GeV}^2$. The ALLM Δ variations with Q^2 are shown in Fig.6. This information is supplemented by inclusive channels like real photoproduction of heavy vector mesons such as J/ψ and $\gamma^* p \rightarrow Vp$, where V stands for a light vector meson.

A summary of HERA new data[14] is presented in Figs.7,8 and 9. $\sigma_{tot}(\gamma^* p)$ data are shown in Fig.7 which displays a dramatic Q^2 dependance. Real photoproduction and small Q^2 data show a very moderate dependance on energy, suggesting that $\Delta \leq 0.1$. As Q^2 is increased the total cross sections become more and more energy dependant making $\Delta \simeq 0.3 - 0.4$ at the highest Q^2 . ALLM lines are added to this figure to guide the eye. A strong energy dependence is also shown in Figs.8 and 9. Fig.8 shows the x dependance of $\sigma(\gamma^* p \rightarrow \rho p)$. The hatched area corresponds to a soft Pomeron prediction and is obviously not adequate. The shaded area corresponds to a PQCD calculation[15]. Fig.9 shows the energy dependance of $\sigma(\gamma p \rightarrow J/\psi p)$. The solid line is a VDM (soft) prediction while the shaded area corresponds to the PQCD calculation of Ryskin[16]. The theoretical ambiguities in Figs.8 and 9 originate from experimental ambiguities in the input gluon density.

The new HERA data indicate clearly the existence of hard Pomeron phenomena with an energy dependance which gets pretty close to the BFKL prediction. Moreover, as is evident from Fig.6 the transition from the soft domain to the hard domain is rather fast. We shall mention here two obvious possible theoretical interpretations of these observations.

1) We have actually two Pomerons. A soft Pomeron with a fixed $\Delta \simeq 0.1$ and a hard BFKL Pomeron with $\Delta \simeq 0.5$. Whereas the small Q^2 data is dominated by the soft Pomeron the higher Q^2 data is dominated by the hard Pomeron. The net effect of the two added contributions is an effective Pomeron whose intercept is Q^2 dependant. Intuitively, such a scenario presumes the decline of the hard Pomeron in kinematic domains that are not accessible to PQCD, and screening suppression of the soft Pomeron at high Q^2 .

2) We have only one soft or semihard Pomeron which, due to PQCD dynamics and screening, develops [17,18] a strong Q^2 dependence. The basic assumption is that the bare Pomeron has $\Delta \simeq 0.25$. For real photoproduction and low Q^2 this value is suppressed due to screening. For higher Q^2 values, the important observation is that the GLAP evolution equations push the value of Δ upward with increasing Q^2 .

In order to differentiate between the above theoretical options and explore some new ones, additional data is needed. To my opinion the key element is to understand the relatively fast transition between $Q^2 = 1\text{GeV}^2$ and 10GeV^2 . Unfortunately, this Q^2 interval is relatively poor with experimental data. These should become available in the near future, and I believe, should help us to resolve the Pomeron mystery.

Acknowledgements: I wish to thank Prof. A. Santoro and my colleagues at LAFEX (CBPF) for their kind hospitality, and the CNPq for financial support. Special thanks to my collaborators E. Gotsman and E.M. Levin.

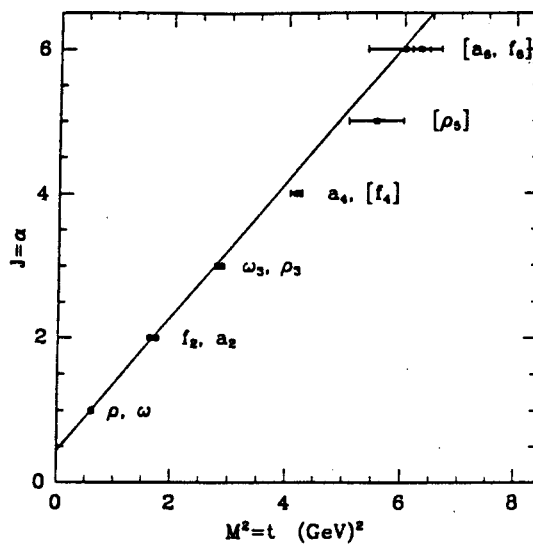


Fig. 1: $\alpha_R(t)$ vs. M^2 , taken from Ref[2].

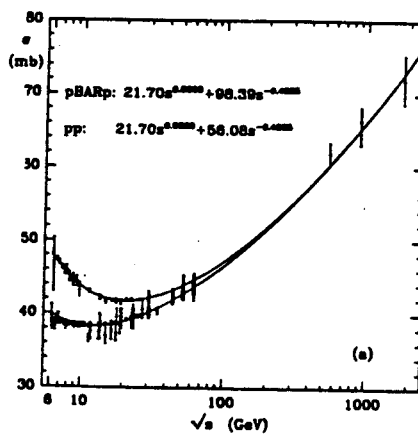


Fig. 2: Total pp and $\bar{p}p$ cross sections fitted by DL[2].

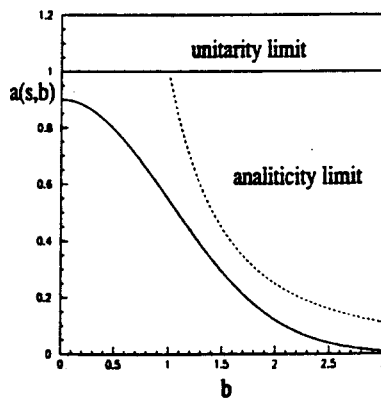


Fig. 3: $a(b,s)$ in impact parameter space.

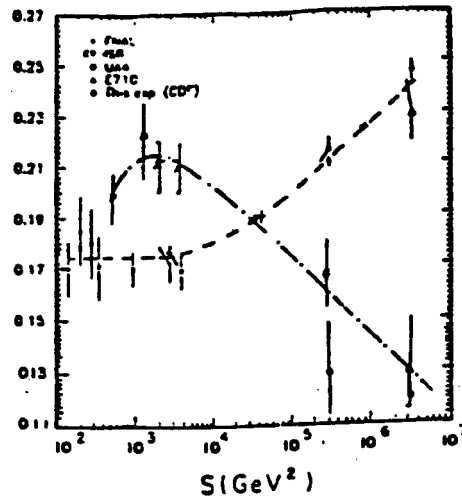


Fig. 4: s dependence of $\frac{\sigma_{el}}{\sigma_{tot}}$ (dashed line) and $\frac{\sigma_{sd}}{\sigma_{tot}}$ (dashed dotted line).

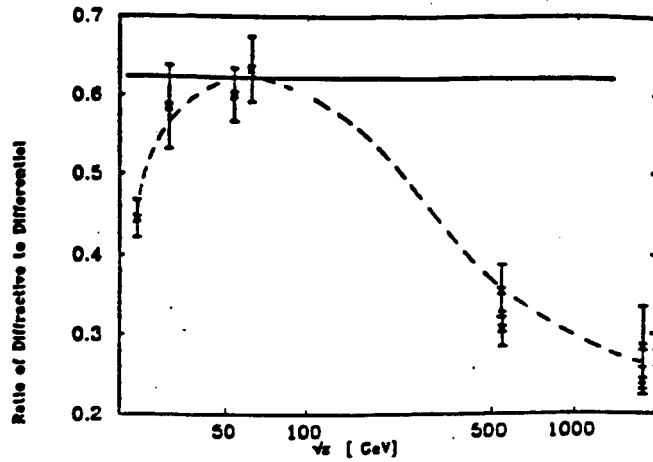


Fig. 5: \sqrt{s} dependence of the ratio between the mass averaged $(\frac{d\sigma_{sd}}{dt})_{t=0}$ and $(\frac{d\sigma_{el}}{dt})_{t=0}$.

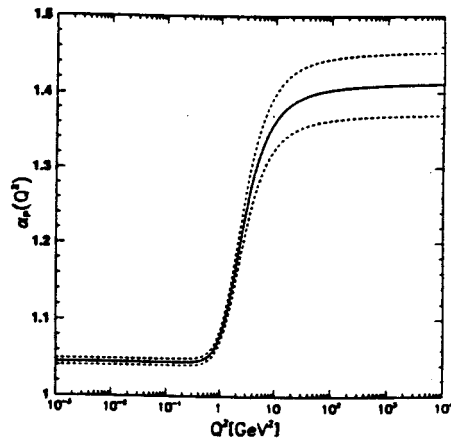


Fig. 6: ALLM Q^2 dependence of the Pomeron intercept $\alpha_P(Q^2)$.

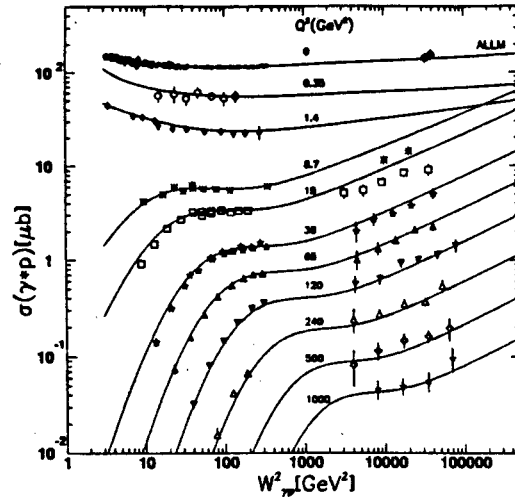


Fig. 7: $\sigma_{tot}(\gamma^*p)$ as a function of the c.m. energy W_{γ^*p} .

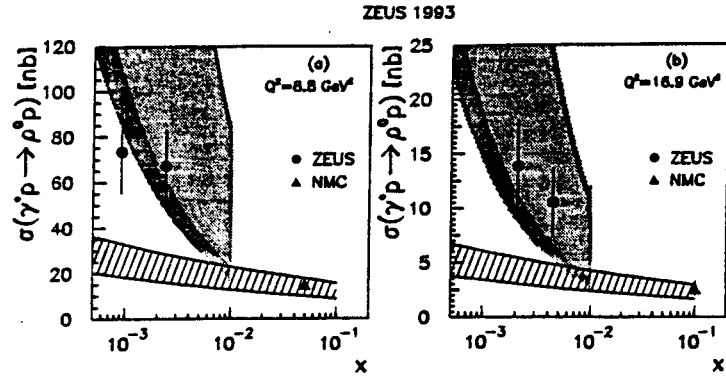


Fig. 8: $\sigma(\gamma^*p \rightarrow \rho p)$ as a function of x .

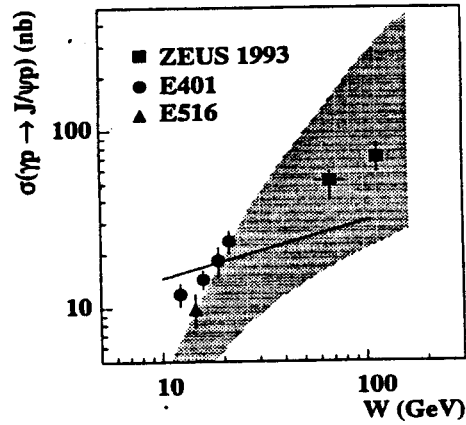


Fig. 9: $\sigma(\gamma p \rightarrow J/\psi p)$ as a function of $W_{\gamma p}$.

References

- [1] P. D. B. Collins, *An Introduction to Regge Theory and High Energy Physics*, Cambridge University Press (1977).
- [2] A. Donnachie and P.V. Landshoff, *Nucl. Phys.* **B231**, (1984) 189; *Phys. Lett.* **B296** (1992) 227.
- [3] M.M. Block, K. Kang and A.R. White, Northwestern University Preprint No. 172 (1992).
- [4] M. Froissart, *Phys. Rev.* **123** (1961) 1053.
- [5] CDF Collaboration, F. Abe et.al., *Phys. Rev.* **D50** (1994) 5518; *ibid*, **D50** (1994) 5535; *ibid* (1994) 5550.
- [6] E. Gotsman, E.M. Levin and U. Maor, *Zeit. Phys.* **C57** (1993) 667.
- [7] E. Gotsman, E.M. Levin and U. Maor, *Phys. Lett.* **B309** (1993) 109.
- [8] E. Gotsman, E.M. Levin and U. Maor, *Phys. Rev.* **D49** (1994) R4321.
- [9] E. Gotsman, E.M. Levin and U. Maor, *Phys. Lett.* **B353** (1995) 526.
- [10] J.D. Pumplin, *Phys. Rev.* **D8** (1973) 2849.
- [11] E. Gotsman, E.M. Levin and U. Maor, *Phys. Lett.* **B347** (1995) 424.
- [12] E.A. Kuraev, L.N. Lipatov and V.S. Fadin, *Sov. Phys. JETP* **44** (1976) 443; *ibid* **45** (1977) 199; Ya.Ya. Balitskii and L.N. Lipatov, *Sov. J. Nucl. Phys.* **28** (1978) 822.
- [13] H. Abramowicz, E.M. Levin, A. Levy and U. Maor, *Phys. Lett.* **B269** (1991) 465.
- [14] ZEUS and H1 collaborations data presented in the VIth Blois Workshop, June 1995.
- [15] S.J. Brodsky et.al., *Phys. Rev.* **D50** (1994) 3134.
- [16] M.G. Ryskin, *Zeit. Phys.* **C57** (1993) 89.
- [17] A. Capella et.al., *Phys. Lett.* **B337** (1994) 358.
- [18] M. Bertini, M. Giffon and E. Predazzi, *Phys. Lett.* **B349** (1995) 561.